Journal of Geophysical Research: Atmospheres

RESEARCH ARTICLE
10.1029/2018JD029089

Enhancing the Fast Radiative Transfer Model for FengYun-4 GIIRS by Using Local Training Profiles

Di Di[1,2,3], Jun Li[4], Wei Han[5], Wenguang Bai[3], Chunqiang Wu[3], and W. Paul Menzel[4]

[1]Chinese Academy of Meteorological Sciences, China Meteorological Administration, Beijing, China, [2]College of Earth Science, University of Chinese Academy of Sciences, Beijing, China, [3]Key Laboratory of Radiometric Calibration and Validation for Environmental Satellites, National Satellite Meteorological Center, China Meteorological Administration, Beijing, China, [4]Cooperative Institute for Meteorological Satellite Studies, University of Wisconsin-Madison, Madison, WI, USA, [5]Numerical Weather Prediction Center, China Meteorological Administration, Beijing, China

Key Points:
- The weighted least squares method improves the accuracy of RTTOV GIIRS simulation over the ordinary least squares method
- Local training profiles improves GIIRS simulation over the global training profiles, which is beneficial to local weather related applications
- The methods can be applied to develop the fast radiative transfer models for sensors onboard the geostationary weather satellites

Correspondence to:
J. Li,
jun.li@ssec.wisc.edu

Citation:
Di, D., Li, J., Han, W., Bai, W., Wu, C., & Menzel, W. P. (2018). Enhancing the fast radiative transfer model for FengYun-4 GIIRS by using local training profiles. *Journal of Geophysical Research: Atmospheres*, *123*, 12,583–12,596. https://doi.org/10.1029/2018JD029089

Received 7 DEC 2017
Accepted 23 OCT 2018
Accepted article online 5 NOV 2018
Published online 19 NOV 2018

Abstract With the successful launch of FengYun-4A (FY-4A), the first satellite in a new Chinese geostationary weather satellite series (FY-4 series), which carries a high spectral resolution infrared (IR) sounder called GIIRS (Geosynchronous Interferometric Infrared Sounder), and vertical atmospheric profiles can be obtained frequently at the regional scale. A fast radiative transfer model is a key component for quantitative applications of GIIRS radiance measurements, including deriving soundings in near real time for situation awareness and radiance assimilation in numerical weather prediction models. The weighted least squares method on enhancing the accuracy of RTTOV (Radiative Transfer for TOVS) for GIIRS is developed. Besides, currently, fast radiative transfer models for IR sensors are based on global training profiles, since GIIRS is targeted for regional observations; it is beneficial for local weather related applications using local training profiles, which better represent the characteristics of that weather regime. A local training profile data set has been developed for GIIRS using the RTTOV approach, comparisons with line-by-line radiative transfer model indicate that weighted least squares method provides better accuracy (smaller root-mean-square error) in the brightness temperature simulation for the middlewave band of GIIRS than the ordinary least squares method, and the local training profiles have further remarkable improvements on brightness temperature simulation over the global training profiles, especially for GIIRS longwave band. The methods can be applied to RTTOV development for other IR sensors onboard the geostationary satellites.

1. Introduction

To improve our knowledge of atmospheric thermodynamics, an effective approach is to use radiance measurements from the high spectral infrared (IR) sounders (or the advanced IR sounders; Menzel et al., 2018), which provide temperature and constituent profiles at a higher accuracy and vertical resolution than the classic IR sounders such as the High-resolution Infrared Radiation Sounder (Smith et al., 1979) and the Geostationary Operational Environmental Satellite (GOES) Sounder (Menzel & Purdom, 1994). The advanced IR sounders, such as the Atmospheric Infrared Sounder (Chahine et al., 2006) onboard the Earth Observing System Aqua platform, the Infrared Atmospheric Sounding Interferometer (IASI) onboard the MetOp-A and MetOp-B satellites (Hilton et al., 2012), and the Cross-Track Infrared Sounder (CrIS) onboard Suomi National Polar-orbiting Partnership and Joint Polar orbit Satellite System series (Goldberg et al., 2013), have proved that the assimilation of radiances from those sounders has a significant positive impact on global and regional numerical weather prediction (NWP; Le Marshall et al., 2006; J. Li et al., 2016; McNally et al., 2014; Wang et al., 2015, 2014, 2017). Similar to IASI and CrIS, the Geosynchronous Interferometric Infrared Sounder (GIIRS) onboard the FengYun-4 (FY-4) series (Yang et al., 2017) is a Fourier transform spectrometer based on a classic Michelson instrument with a 0.8-cm^{-1} maximum optical path difference. The GIIRS spectral range is divided into two bands, with band 1 (longwave band) ranging from 700 to 1,130 cm^{-1} and band 2 (middlewave band) ranging from 1,650 to 2,250 cm^{-1}. Band 1 is mainly designed for atmospheric temperature and ozone sounding, while band 2 is used primarily for atmospheric humidity sounding. With a unapodized spectral resolution of 0.625 cm^{-1}, the two bands have 689 and 961 channels, respectively. Unlike the first three advanced IR sounders, which are in polar orbit, GIIRS is the first high spectral resolution advanced IR sounder onboard a geostationary weather satellite. Launched on 11 December 2016, FY4A is the

first satellite among the second generation of the Chinese geostationary weather satellite series; the remaining satellites of this series are planned to be launched from 2019 to 2025 and beyond (Yang et al., 2017). Since severe weather warning, nowcasting and short-term forecasting require nearly continuous monitoring of the vertical temperature and moisture structure of the atmosphere (Schmit et al., 2009), and since GIIRS has an unprecedented advantage to observe the fast-changing water vapor and temperature structures related to severe weather events (J. Li et al., 2011, 2012), FY4A will provide vital information necessary for enhancing nowcasting and NWP services, for example, improve local severe storm short range forecast via data assimilation (Z. Li et al., 2018). Besides the GIIRS sensor, the two other main advanced instruments onboard the FY-4A platform are the Advanced Geosynchronous Radiation Imager (AGRI) and Lightning Mapping Imager. Together, they provide important measurements for applications on severe weather monitoring, warning, and forecasting.

For most applications of satellite-based IR radiances for NWP, notably satellite data assimilation and atmospheric profile retrieval, an accurate and fast radiative transfer model (RTM) is required to simulate radiances with specific atmosphere profiles as input. The most widely used fast RTMs in the world are represented by the Radiative Transfer for TOVS (RTTOV) model developed by the NWP Satellite Application Facility from European Organisation for Exploitation of Meteorological Satellite (Eyre, 1991; Matricardi et al., 2001; Saunders et al., 1999) and the Community Radiative Transfer Model developed by National Oceanic and Atmospheric Administration's (NOAA) Joint Center for Satellite Data Assimilation (Chen et al., 2010, 2008). The core of fast RTM is a fast transmittance calculation (transmittance model) that is parameterized by a database of accurate line-by-line (LBL) transmittances computed from a set of diverse atmospheric profiles, which makes the fast RTM computationally efficient and of high accuracy (Matricardi, 2008) for applications. Therefore, one of the important factors that affect the uncertainty of fast RTM radiance simulation is the high spectral resolution transmittance database produced from diverse atmospheric profiles with an LBL model, along with a parameterization scheme for fast transmittance calculation. Research has been conducted on the enhancement and assessment of the RTTOV model, including assessing the accuracy of different LBL models (Matricardi, 2005, 2008), improving the parameterization scheme (Matricardi, 2008), and selecting a new set of global profiles for the transmittance database (Matricardi, 2008). In general, the set of training profiles used as input to various LBL models is chosen to represent the range of variation in both atmospheric temperature and constituents in the global atmosphere. Because GIIRS sounder only covers a specific region, a set of regional or local training profiles can better represent the atmospheric conditions within the FY-4A GIIRS observation coverage. It makes more sense to use local training profiles in a fast RTM for the geostationary advanced IR sounder, especially for regional weather applications.

This study focuses on (1) enhancing and assessing RTTOV GIIRS with weighted least squares (WLS) method and (2) developing local training profiles for RTTOV GIIRS built on the methodology from (1). The first part of this paper is to develop a new methodology for generating the fast model coefficients for any IR sensor, while the second part of the paper is to develop the local training profiles for RTTOV GIIRS coefficients built on the selected methodology from the first part. In the first part, the WLS method on improving the accuracy of RTTOV coefficients is developed and selected. In the second part, the local training profiles are developed and show improvements on the brightness temperature (BT) simulation over the global training profiles, which is beneficial to local weather related applications when using GIIRS measurements. The method can be applied to develop the fast RTMs for IR bands of geostationary imagers such as the Advanced Baseline Imager onboard the GOES-R series (Schmit et al., 2005), the Advanced Himawari Imager onboard Himawari-8/-9 (Bessho et al., 2016), and the AGRI onboard FY-4 series (Yang et al., 2017) and sounders such as the current GOES Sounder, the GIIRS onboard the FY-4 series, and the InfraRed Sounder onboard future Meteosat Third Generation series, for local weather related applications such as data assimilation in NWP models, and efficient profile retrieval (J. Li et al., 2000; J. Zhang et al., 2014; K Zhang et al., 2016) for situation awareness and nowcasting.

This paper is organized as follows. The RTMs and profile database used in the study are described in section 2. The regression methods adopted for enhancing the fast RTM using the common global training profiles, along with the evaluations are explained in section 3. The method for further enhancing the fast RTM for GIIRS using local training profiles, along with the assessment, is described in section 4. Summary and future works are given in section 5.

2. Training Data Set and RTMs

2.1. Database

Both local and global training profiles are used to generate two versions of RTTOV regression coefficients for GIIRS, respectively. The global training profile data set contains 83 profiles generated at the European Centre of Medium-Range Weather Forecasts (ECMWF) by Matricardi (2008), which are sampled from a large profile database described in Chevallier et al. (2006). The global training profiles have been widely used for generating coefficients for various satellite sensors at ECMWF for satellite data assimilation. The other profile database, called SeeBor Version 5.0 (Borbas et al., 2005) and was created at the Cooperative Institute for Meteorological Satellite Studies (CIMSS) of the University of Wisconsin-Madison, consists of 15,704 global atmospheric profiles of temperature, moisture, and ozone at 101 pressure levels for clear-sky conditions. The profiles are generated from several databases, including NOAA-88, an ECMWF 60-L training set, TIGR-3, ozonesondes from eight NOAA Climate Monitoring and Diagnostics Laboratory sites, and radiosondes from 2004 in the Sahara desert. The SeeBor Version 5.0 database used here is mainly for producing a set of local training profiles based on the atmospheric characteristics of the FY4A GIIRS observation coverage. In addition, independent test profiles for assessing the simulation accuracy of RTTOV GIIRS regression coefficients are also selected from the SeeBor Version 5.0 database.

2.2. RTMs

RTTOV is a fast RTM for TOVS originally developed at ECMWF in the early 1990s (Eyre, 1991). Subsequently, the codes have gone through several updates (Matricardi et al., 2001; Saunders et al., 1999), more recently within the European Organisation for Exploitation of Meteorological Satellite NWP Satellite Application Facility. RTTOV v11.2 is the version adopted here. An important feature of the RTTOV model that is essential for NWP is that it provides not only fast and accurate calculations of the forward radiances but also fast computation of the Jacobian matrix, which are the partial derivatives of the channel radiances with respect to the model input variables, such as temperature and gas concentration that influences those radiances (Chen et al., 2010).

As discussed, the RTTOV fast transmittance algorithm requires accurate transmittances from an LBL model. The LBL model selected in this study is version 12.6 of the line-by-line radiative transfer model (LBLRTM) developed at Atmospheric and Environmental Research Inc. and derived from the Fast Atmospheric Signature Code (Clough et al., 1989, 1981, 1992, 2005). To describe the effects of pressure and Doppler line broadening, the Voigt line shape is calculated at all atmospheric levels, which provides the foundation for the LBLRTM line shape. Requisite modifications to the Voigt line shape have been implemented based on analyses of laboratory and atmospheric spectra including line coupling and the water vapor continuum (Clough et al., 2005; Matricardi, 2008, 2009). LBLRTM provides spectral radiance calculations with high accuracies and that are consistent with the measurements against which they are validated. As described in Matricardi (2007), the LBL model errors mainly come from insufficient knowledge of basic spectroscopy rather than the computational scheme adopted in the codes.

3. Methodologies for RTTOV GIIRS With Global Training Profiles

3.1. Generation of RTTOV GIIRS Global Coefficients

A prerequisite for RTTOV model forward simulation is generating the regression coefficients for various sensors. To generate RTTOV global coefficients for GIIRS, an accurate monochromatic transmittance database calculated from a set of global diverse atmospheric profiles over the GIIRS spectral range is needed. The global training profiles used here are explained in section 2.1 above. The monochromatic transmittance database first generated from the LBLRTM will then be convolved with the appropriate GIIRS instrument spectral response function (SRF) to obtain corresponding channel transmittances, which become the data points in the regression. Finally, the regression coefficients (RTTOV GIIRS global coefficients) are produced by a selected set of predictors, which are called as v7 predictors in the RTTOV model (Matricardi & Saunders, 1999).

Note that the v7 predictors mainly relate to the variable as temperature, humidity, and ozone concentration. Only H_2O and O_3 are treated as variable gases in this version of RTTOV GIIRS model. Besides, there are several points stated why hamming apodization is applied to the GIIRS interferograms. Generally, interferograms

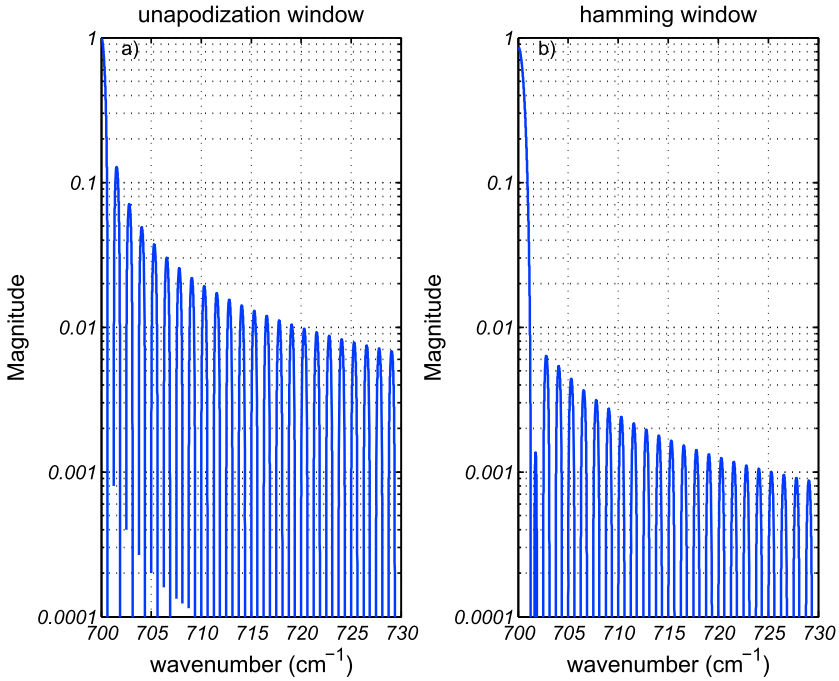

Figure 1. The illustration of the hypothetical spectral response function of the Geosynchronous Interferometric Infrared Sounder over 700 cm^{-1} applying the (a) unapodization window and (b) hamming window.

such as IASI and CrIS will be applied with apodization window to produce a channel response function that is localized and has small side lobes. And the hamming apodization is used in that the inverse transformation can be used to readily convert computed hamming apodized spectra to spectra computed for other apodization functions. So the SRF of the GIIRS instrument used for simulation is equal to the inverse Fourier transform of a hamming function which has been truncated with a 0.8 cm^{-1} maximum optical path difference. Take the SRF of the GIIRS instrument over 700 cm^{-1} as an illustration. It can be seen from Figure 1 that spectral crosstalk of SRF will be substantially decreased by adding the hamming apodization window than unapodizated.

The last key step of generating RTTOV GIIRS global coefficients is to solve a multiple linear regression problem. It is common to consider adopting the least squares method for a regression problem. One disadvantage of ordinary least squares (OLS) method is that its estimates can behave badly when the residual error distribution is not normal. Mostly, 83 training profiles with six viewing angles (the secant varies from 1 to 2.25 with an interval of 0.25) will produce 498 samples for each regression. However, quite meaningless negative channel transmittances are created by the LBLRTM or in the procedure of convolution, especially for the channels detecting upper atmosphere. It may turn to be a linear regression problem with small samples for certain channels, which implies the effect of abnormal data on regression accuracy will be intensified in this case. The WLS method (robust regression) is considered here for its feature on eliminating the overlarge influence of abnormal data. In addition, threshold value method (limit the transmittances used in the regression by threshold value) is also to be tested since it may have the similar role on abnormal data.

The WLS method (robust regression) is to use a fitting criterion that is not as sensitive as OLS method to abnormal data and influential points, which is also known as M-estimation that introduced by Huber (1964). This WLS method has a high level of robustness and can be regarded as a generalization of maximum-likelihood estimation (Fox & Weisberg, 2011). Assuming the linear model for *i*th of *n* observations:

$$y_i = \beta_0 + \beta_1 x_{i1} + \beta_2 x_{i2} + \cdots + \beta_m x_{im} + \varepsilon_i = x_i{}^T \beta + \varepsilon_i \quad (1)$$

Given an estimator *b* for β, equation (1) is equal to

$$\hat{y}_i = b_0 + b_1 x_{i1} + b_2 x_{i2} + \cdots + b_m x_{im} + e_i = x_i{}^T b \tag{2}$$

where e_i is the residuals given by $e_i = y_i - \hat{y}_i$. For M-estimation, the estimates b are determined by minimizing the particular objective function:

$$\sum_{i=1}^{n} \rho(e_i) = \sum_{i=1}^{n} \rho\left(y_i - x_i^T b\right) \tag{3}$$

where function ρ should meet the following requirements: (1) nonnegative, (2) equal to 0 when its argument is 0, (3) symmetric, and (4) monotone; if differentiating the objective function with respect to the coefficients b and setting the partial derivatives to 0, equation (3) can be changed as

$$\sum_{i=1}^{n} \psi\left(y_i - x_i^T b\right) x_i^T = 0 \tag{4}$$

where ψ is the derivation of ρ and ψ is called the influence curve. For simplicity, define the weight function $w(e) = \psi(e)/e$, equation (4) can be written as

$$\sum_{i=1}^{n} w_i \left(y_i - x_i{}^T\right) x_i^T = 0 \tag{5}$$

Therefore, the problem is equivalent to a WLS problem. From description above, it is obvious that the estimated coefficients depend on the weights, while the weights rely on the residuals and the residuals rely on the estimated coefficients. An iterative solution using following steps is required to get the estimated coefficients:

1. Obtain the initial estimates $b^{(0)}$and residual $e^{(0)}$, it is generally obtained by the OLS method.
2. Calculate the initial weighting function $w^{(0)}$with residual $e^{(0)}$.
3. Solve for new WLS estimates by the equation $b^{(1)} = (X^T W_0 X)^{-1} X^T W_0 Y$
4. Calculate the new residual $e^{(1)}$and weighting function $w^{(1)}$
5. Repeat the steps 3 and 4 until the estimated coefficients converge.

Frequently used objective functions for M-estimators contain least squares function, Huber function and bisquare function. In this study, the bisquare function is adopted and its expression is

$$\rho(e) = \begin{cases} \dfrac{k^2}{6}\left\{1 - \left[1 - \left(\dfrac{e}{k}\right)^2\right]^3\right\} & \text{for} |e| \leq k \\ k^2/6 & \text{for} |e| > k \end{cases} \tag{6}$$

in which e is the residual and k is called a tuning constant. Tuning constants give coefficients estimates that are approximately 95% as statistically efficient as the OLS estimates, provided that the response has a normal distribution with no outliers. We use $k = 4.685\sigma$ for the bisquare, where σ is the standard deviation of the errors and σ = MAR/0.6745, where MAR is the median absolute residual.

Next, four schemes are carried out to study the impact of different regression methods on BT simulation accuracy:

Scheme 1: OLS method or OLS for simplicity,
Scheme 2: OLS method + threshold value or OLS + threshold for simplicity,
Scheme 3: WLS method or WLS for simplicity, and
Scheme 4: WLS method + threshold value or WLS + threshold for simplicity.

The accuracy of RTTOV forward BT simulations is assessed by comparisons between RTTOV GIIRS with global training profile using the above four schemes, respectively, and LBLRTM calculations. When simulating the channel radiances from LBLRTM, the radiance spectrum will be convolved with the same SRF used in the calculation of channel transmittances. As a rule, the accuracy of a fast RTM model simulation is quantified by the bias and root-mean-square error (RMSE) using LBLRTM calculations as references (true). Usually, there are two different ways for evaluating a fast RTM (Saunders et al., 1999), one is called dependent evaluation that uses

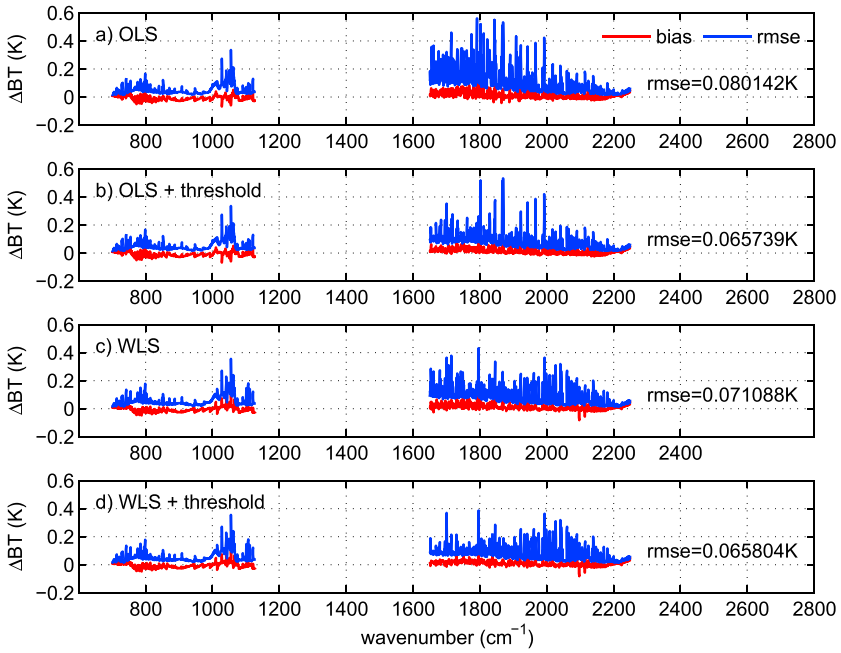

Figure 2. Mean bias and RMSE (unit: K) of the BT simulation differences between RTTOV Geosynchronous Interferometric Infrared Sounder and line-by-line radiative transfer model tested by dependent training profiles at six viewing angles with the RTTOV coefficients generated from European Centre of Medium-Range Weather Forecasts 83 global training profiles; (a–d) use the coefficients created by OLS method, OLS + threshold method, WLS method, and WLS + threshold, respectively. BT = brightness temperature; OLS = ordinary least squares; RMSE = root-mean-square error; WLS = weighted least squares; RTTOV = Radiative Transfer for TOVS.

the same profiles in generating the RTTOV coefficients for evaluation, while another one is called independent evaluation that uses randomly selected profiles out of the profiles in generating the RTTOV coefficients for evaluation. Evaluations of four schemes with dependent training profiles at six viewing angles are shown in Figure 2. It shows that both the threshold value method and WLS method have larger improvements on BT simulation accuracy than the OLS method, especially for the middlewave band. The OLS + threshold method and WLS + threshold method perform best over the entire GIIRS spectrum. The major improvements from the threshold value method than the OLS method are mainly found around 1,650- to 1,900-cm^{-1} spectral region associated with strong water vapor absorption lines. The main improvements from WLS method are also found from 1,650- to 1,900-cm^{-1} spectral region that contains most water vapor channels of GIIRS. However, Figure 2c reveals the WLS method preforms relatively poorly for the 2,000- to 2,100-cm^{-1} spectral region. The results are from dependent comparisons using the same global training profiles; the independent comparisons are further conducted below.

3.2. Independent Evaluation of RTTOV GIIRS Global Coefficients

Assessing the performance of global coefficients requires adequate testing profiles that are independent of the training profiles. The FY-4A GIIRS is designed primarily for detecting the atmospheric vertical structure over the China and its adjacent regions (15°–55°N, 70°–140°E) continuously. Considering the fact that the atmospheric profiles commonly vary with latitudes, the whole region for selecting the testing profiles is divided into four latitudes, which are labeled as Lat1 (15°–25°N, 70°–140°E), Lat2 (25°–35N, 70°–140°E), Lat3 (35°–45°N, 70°–140°E), and Lat4 (45°–55°N, 70°–140°E), respectively. Accordingly, 50 independent testing profiles located within each of the four latitudes are randomly chosen from the CIMSS SeeBor Version 5.0 database. There are a total of 1,200 samples (200 test profiles and 6 corresponding viewing angles) used for evaluation on BT simulation accuracy.

Evaluations of the four schemes for the forward BT simulation accuracy with independent testing profiles are exhibited in Figure 3. Same conclusions could be drawn that the OLS + threshold method, the WLS method, and the WLS + threshold method have better performance than the OLS method, which has a 10.87%,

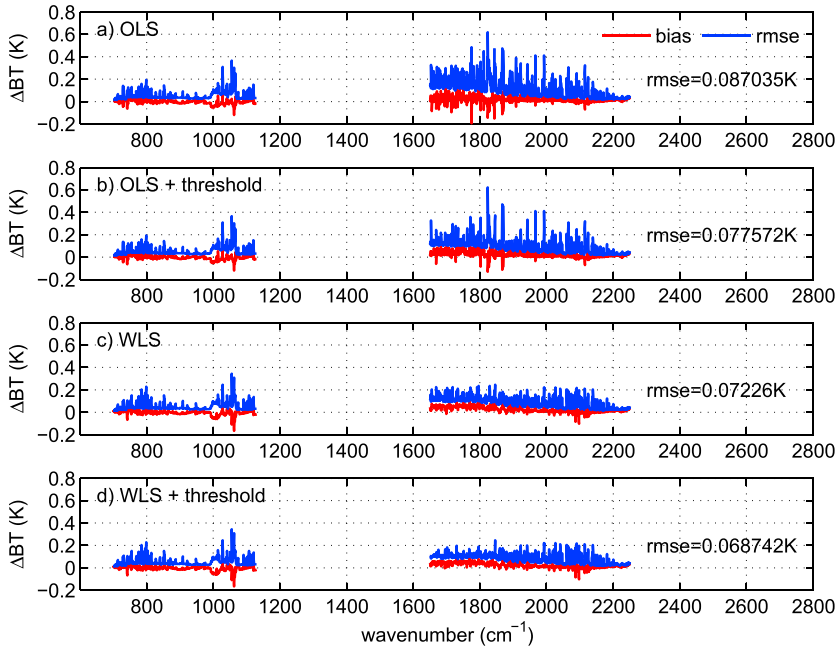

Figure 3. Mean bias and RMSE (unit: K) of the BT simulation differences between RTTOV Geosynchronous Interferometric Infrared Sounder and line-by-line radiative transfer model assessed by 200 independent testing profiles at six viewing angles with the RTTOV coefficients generated from European Centre of Medium-Range Weather Forecasts 83 global training profiles; (a–d) use the coefficients created by OLS method, OLS + threshold method, WLS method, and WLS + threshold, respectively. BT = brightness temperature; OLS = ordinary least squares; RMSE = root-mean-square error; WLS = weighted least squares; RTTOV = Radiative Transfer for TOVS.

16.98%, and 21.02% improvement on BT simulation accuracy, respectively, over the entire GIIRS spectrum. Similarly, the major improvements are mainly found over middlewave band. For middlewave band only, there are 14.53%, 21.56%, and 26.96% improvements on BT simulation accuracy, respectively. However, Figure 3b reveals that the OLS + threshold method does not perform as good as that from the dependent training profiles, although its performance is still superior to the OLS method. It implies that the threshold value method lacks robustness and cannot effectively substitute the WLS method. The WLS method performs well for the most spectral regions of middlewave band, even for 2,000-to 2,100-cm^{-1} spectral region where it does not work very well on dependent training profiles, and its performance is comparable to OLS + threshold method. Figure 3d shows that the WLS method will have better performance if it is combined with a reasonable threshold value.

Based on both the dependent and independent evaluations, it could be drawn that the WLS method or WLS + threshold method is the most recommended approach for generating the sensor coefficients for RTTOV model, although neither approach performs best for every channel. This method (WLS or WLS + threshold) can be applied for generating RTTOV coefficients for any IR sensor onboard either polar orbit or geostationary satellites. However, some limitations (e.g., does perform the best for every channel) linked to the WLS method should be further studied, which will be our next research focus.

4. Methodologies for RTTOV GIIRS With Local Training Profiles

4.1. Development of Local Training Profiles for RTTOV GIIRS

GIIRS, as a geostationary advanced IR sounder, only observes a specific region (15°–55°N, 70°–140°E), so the representation of global training profiles used for developing RTTOV GIIRS might not be optimal for regional applications. The analyses on the comparison between using global training profiles and regional training profiles are needed. In order to select the representative local training profiles, the selected region (10°–60°N; 50°–160°E; labeled as local region) has been expanded from actual FY-4A GIIRS observation coverage. All the profiles of the SeeBor Version 5.0 database (hereafter referred to as global profiles) are counted

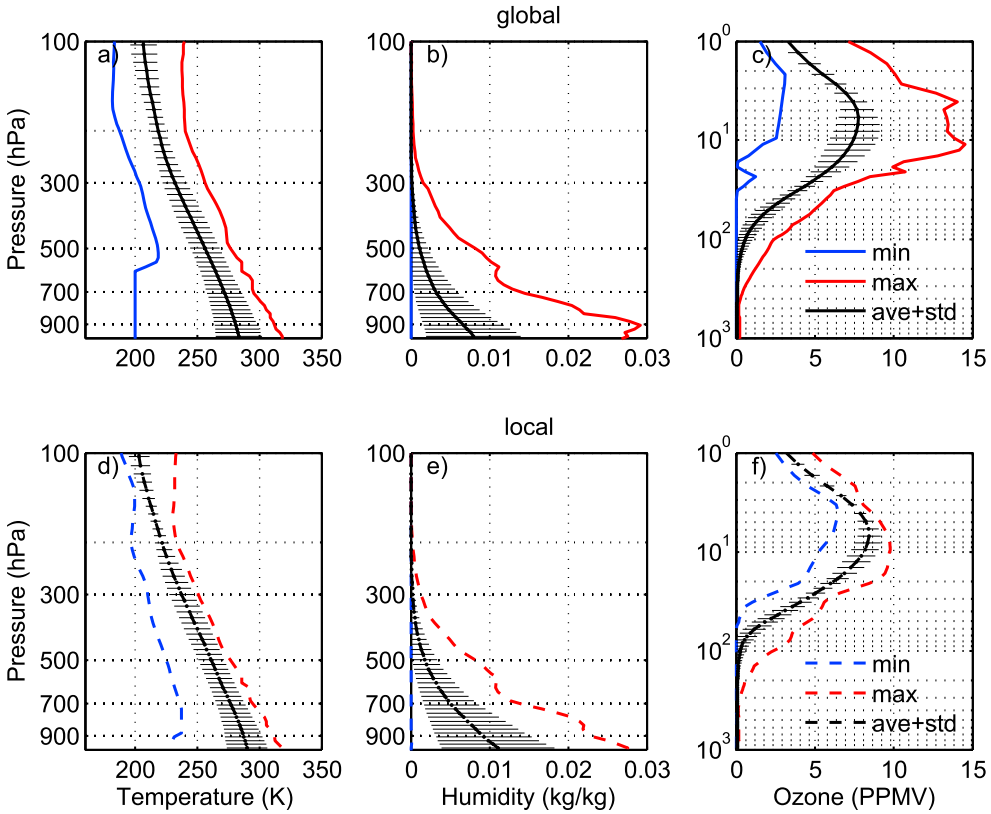

Figure 4. Statistics of temperature, water vapor, and ozone profiles within global and local region, respectively. The minimum, mean, and maximum values of global profiles are shown in blue, black, and red solid lines. The minimum, mean, and maximum values of local profiles are shown in blue, black, and red dashed line. The mean value is attached by a width of twice the standard deviation.

for the statistics of global atmospheric parameters, while the profiles located within the local region (hereafter referred to local profiles) are calculated for the statics of local atmospheric parameters. This analysis primarily focuses on the comparison of parameters such as temperature, humidity, and ozone content. The statistic results of three parameters specific to two regions (global and local) are plotted in Figure 4. The minimum, mean, and maximum values of global profiles and local profiles are shown in blue, black, and red solid lines and dashed lines, respectively. Obviously, the local profiles tend to be warmer and wetter than global profiles. And the variation range of temperature, humidity, and ozone of local profiles is smaller. The differences of ozone concentration between two regions are largest including its variation range and variability. In our opinion, a set of local training profiles will be better representing the atmospheric conditions within the GIIRS observation coverage. It makes more sense to use local training profiles in fast RTM for a geostationary advanced IR sounder.

The sampling strategy adopted in this research is called the constrained random selection method, which has been documented by Matricardi (2008) and Chevallier et al. (2006). The method has been adjusted appropriately for RTTOV GIIRS development, and the modified sampling strategy for local training profiles has three steps. The first step is to select the initial local training profiles from the ECMWF 83 global training profiles based on local region (10°–60°N; 50°–160°E). A total of 14 profiles is selected in the first step; these profiles are illustrated by the black dots in Figure 5.

The second step is to select the candidate profiles to be added into the initial local training profiles. With an iterative approach based on the Euclidean distance quantity that measures the dissimilarity between two atmospheric profiles, a set of candidate profiles are chosen using this iterative approach: The first atmospheric profile is randomly taken from the SeeBor Version 5.0 database, and an alternative profile in the remaining database is then taken if it has the largest Euclidean distance among the already selected profile

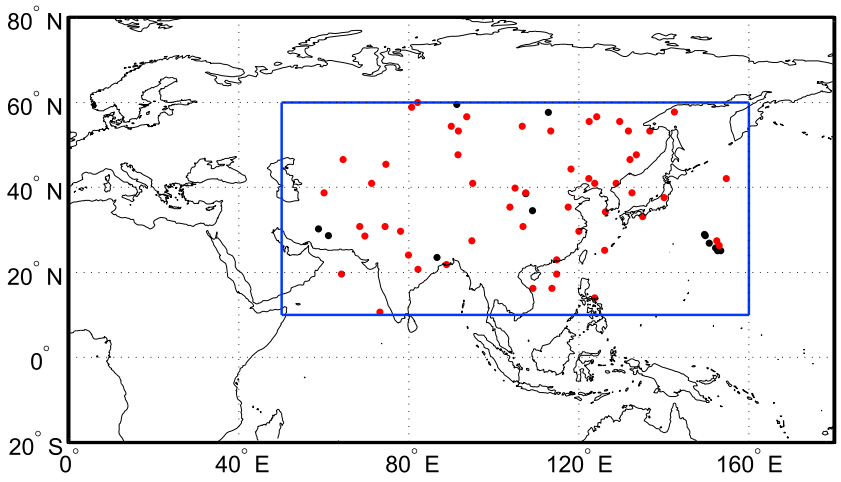

Figure 5. Geographical distribution of the 70 local training profiles. Black and red dots denote training profiles sampled from the European Centre of Medium-Range Weather Forecasts 83 profile database and Cooperative Institute for Meteorological Satellite Studies SeeBor profile database, respectively. Blue rectangle marks the selected region of local training profiles.

set; repeat this procedure until enough candidate profiles are selected. It is apparent that the size of the collected profiles can be controlled based on the cycle index. The Euclidean distance is defined as follows:

$$D = \mathrm{Min}\sqrt{\sum_{l=1}^{N}\left(\frac{\theta_i(l)-\theta_j(l)}{\sigma_\theta(l)}\right)^2} \tag{7}$$

where $\theta_i(l)$and $\theta_j(l)$ represent the variable at pressure level l for profile i (alternative profile) and j (already selected profile), respectively; Involved variables include temperature, specific humidity, and specific ozone;$\sigma_\theta(l)$ is the standard deviation of $\theta_j(l)$. The above approach has been applied to sample the temperature profiles, the humidity profiles, and the ozone profiles, respectively, and the size of each independent profile set has been limited to a total of 500. A candidate database made of 1265 profiles from local region has been created after mixing the three separated sets of profiles.

The last step is to constrain the random profiles selection from candidate database. As suggested in Matricardi (2008), it is necessary to have the training profiles at each pressure level to be distributed as uniformly as possible across the range covered by the profiles for optimizing the distribution of LBL transmittances used in the regression. In addition to the 14 initial local training profiles selected from the global training profiles, an additional 53 training profiles are further selected from the 1,265 candidate profiles. Considering all the possible random permutation of 1,265 profiles, taking 53 at a time is too computationally expensive to be conducted, the number of random permutations is limited to 10^8. The selection process is as follows: In each loop, 53 additional profiles are randomly taken from the 1,265 candidate profiles, and they are combined with the already selected initial 14 training profiles to form the local training profiles; then all the temperature profiles, water vapor profiles, and ozone profiles of this local training set are divided into 67 bins at each pressure level. For each pressure level i, the number of profiles $N_{ij}^{\mathrm{Temperature}}$, $N_{ij}^{\mathrm{Watervapor}}$, and N_{ij}^{Ozone} are computed in each bin j and the sum N is obtained using the following formula:

$$N = \sum_{i=1}^{101}\sum_{j=1}^{67}\left|\left(N_{ij}^{\mathrm{Temperature}}-1\right)\right| + \sum_{i=1}^{101}\sum_{j=1}^{67}\left|\left(N_{ij}^{\mathrm{Watervapor}}-1\right)\right| + \sum_{i=1}^{101}\sum_{j=1}^{67}\left|\left(N_{ij}^{\mathrm{Ozone}}-1\right)\right|; \tag{8}$$

In all the 10^8 loops, the ensemble of the profiles with the minimum value of N is the optimal set. In addition, two profiles (minimum and maximum of 67 profiles) are added after the automatic selection of 53 profiles as well as one more profile that computed as the average of the 69 profiles. Finally, there are 70 local training profiles selected in total for generating the RTTOV GIIRS local coefficients. The geographical distribution of the 70 local training profiles is shown in Figure 5, where the red dots denote local profiles sampled from the CIMSS SeeBor global profile database.

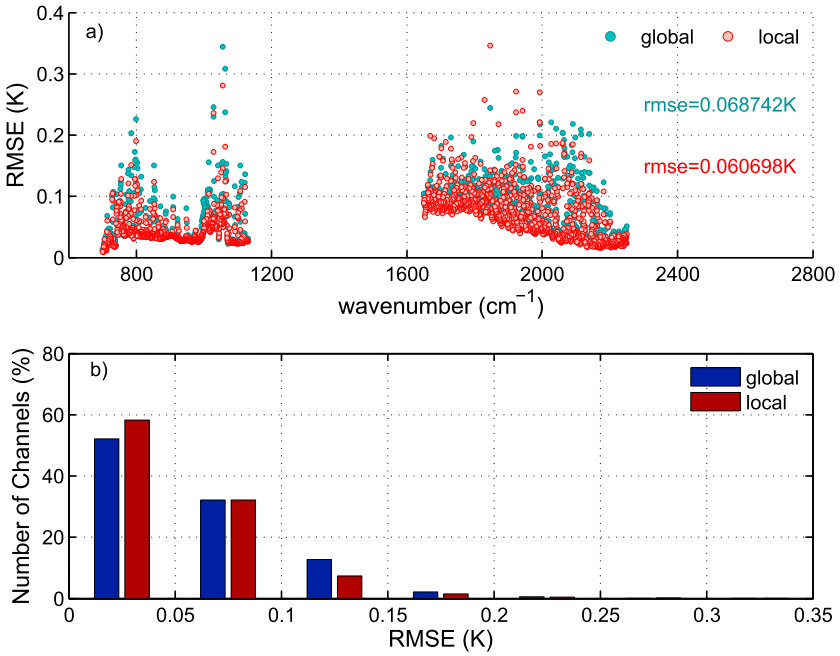

Figure 6. (a) Mean RMSE (unit: K) of the brightness temperature simulation between global coefficients and local coefficients (scheme 4) over the entire Geosynchronous Interferometric Infrared Sounder spectrum accessed by 200 independent testing profiles at six viewing angles. The green dots and red dots represent the RMSEs of global coefficients and local coefficients, respectively. (b) Number of channels (unit: %) meeting the accuracy requirements (seven RMSE thresholds) based on mean RMSE of brightness temperature simulation using global coefficients and local coefficients accessed by 200 independent testing profiles. RMSE = root-mean-square error.

It should be noted that 200 testing profiles used above are excluded in the process of choosing local training profiles to ensure that the testing profiles are absolutely independent of local training profiles.

4.2. Performance of RTTOV GIIRS Local Coefficients

The procedure of generating RTTOV GIIRS local coefficients is similar to that of global coefficients, which has been explained in section 3.1 above. Unlike the ECMWF 83 global profiles used in RTTOV GIIRS global coefficients, the 70 local training profiles described above are used to generate the RTTOV local coefficients. Other sets such as GIIRS instrument SRF and regression predictors are kept consistent between global and local coefficients.

Evaluations for RTTOV GIIRS local coefficients created by four schemes with 200 independent testing profiles and six viewing angles are also conducted (results not shown). Likewise, the OLS + threshold method, WLS method, and WLS + threshold method all have better performance than OLS method; besides, the WLS + threshold method makes even larger improvement over other methods for local coefficients than global coefficients. It indicates that WLS + threshold method performs better for local training profiles with smaller sample size.

In order to understand the superiority of local training profiles over the global training profiles for GIIRS RTTOV BT simulation, the evaluation is focused on the BT comparisons between using local coefficients and global coefficients with WLS + threshold method (Scheme 4 in section 3), since the WLS + threshold method performs best overall based on the dependent and independent evaluations mentioned in section 3. Again, the LBLRTM BT calculations are used as references (true) in the comparisons. RMSEs of BT differences between RTTOV GIIRS and LBLRTM are calculated from 200 independent testing profiles at six viewing angles (see Figure 6a); overall, the BT simulation accuracy of local coefficients is higher than that of global coefficients with a 11.70% improvement. For the longwave band, the improvements from local coefficients are remarkable, and the larger ones occur in the spectral regions around 800 cm^{-1} associated with CO_2 lines, and 1,050 cm^{-1} associated with O_3 lines. For the middlewave band, the improvements

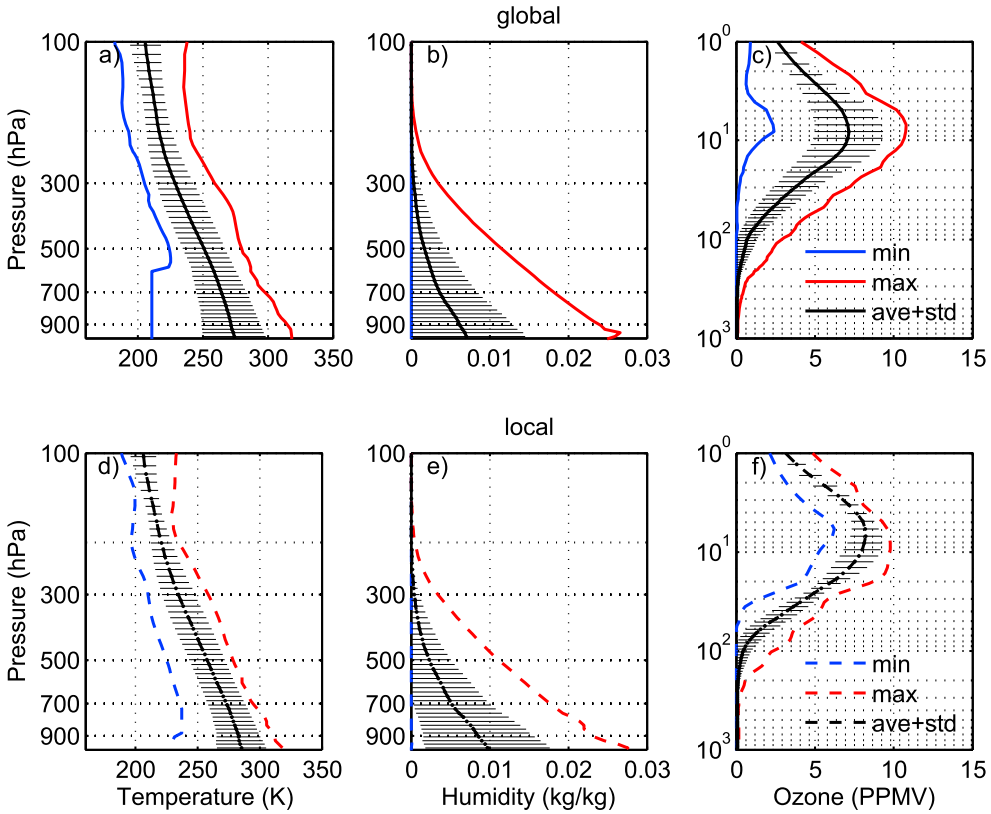

Figure 7. Statistics of atmospheric temperature, water vapor, and ozone of global training profiles and local training profiles, respectively. The minimum, mean, and maximum values of global training profiles are shown in blue, black, and red solid lines. The minimum, mean, and maximum values of local training profiles are shown in blue, black, and red dashed lines. The mean value is attached by a width of twice the standard deviation.

from local coefficients are founded from 1,900- to 2,100-cm^{-1} spectral region associated with interfering H_2O, N_2O, and CO lines. Figure 6b shows the number of channels meeting the accuracy requirements (seven RMSE thresholds) based on mean RMSE of BT differences between global coefficients and local coefficients, respectively, from 200 testing profiles at six viewing angles. Seven RMSE thresholds range from 0.05 to 0.35 K with an interval of 0.05 K. It can be seen that there are more channels meeting the 0.05-K accuracy standard with local coefficients than with global coefficients, which also indicates the superiority of local coefficients for GIIRS RTTOV.

For further analysis of the difference between global training profiles and local training profiles, statistical comparisons of temperature, water vapor, and ozone concentration between global training profiles and local training profiles are displayed in Figure 7. For temperature and ozone, the differences between local training profiles and global training profiles are relatively obvious, which is consistent with the results in Figure 4. The statistic patterns of temperature and ozone of local training profiles are closer to overall characteristics of profiles located within local region, which might be the main reason that there is a better performance on temperature and ozone channels with local coefficients. It should be noted that the BT simulation accuracy of several channels with central wavenumbers around 1,850 cm^{-1} is distinctly lower from local coefficients. These channels can be excluded in the applications of GIIRS observations (e.g., in NWP assimilation and atmospheric profile retrieval). In order to further understand the improvement from local training profiles, the independent testing profiles are divided into four latitudes regions, which are labeled as Lat1 (15°–25°N, 70°–140°E), Lat2 (25°–35°N, 70°–140°E), Lat3 (35°–45°N, 70°–140°E), and Lat4 (45°–55°N, 70°–140°E), respectively. There are 50 independent testing profiles in each latitude region. The BT simulation accuracies of global and local coefficients for the four latitudes are shown in Figure 8, using again the LBLRTM BT calculations as references (true). It can be seen that the BT simulation accuracy of local coefficients is higher than that of global coefficients no matter in which latitude region. Local coefficients

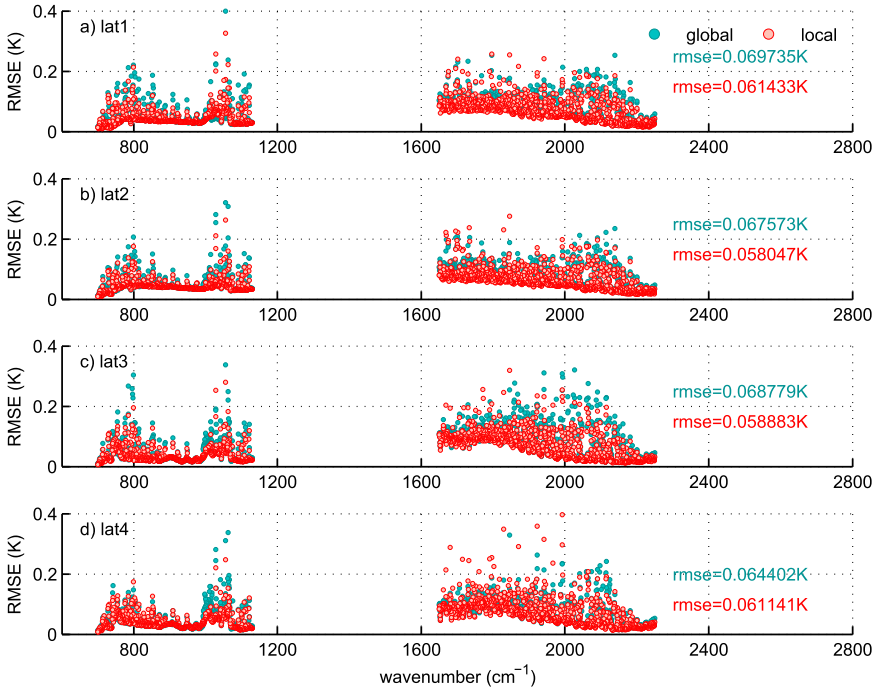

Figure 8. Mean RMSE (unit: K) of the brightness temperature simulation using local coefficients and global coefficients over the entire Geosynchronous Interferometric Infrared Sounder spectrum assessed by the independent testing profiles from four different latitude regions. RMSE = root-mean-square error.

have a 11.9%, 14.10%, 14.39%, and 5.06% improvement over global training coefficients on BT simulation accuracy for the four latitudes, respectively. The improvements from local coefficients over global coefficients for Lat2 and Lat3 are more remarkable than those for Lat1 and Lat4, which implies the local coefficients perform better for profiles in the nonextreme atmospheric conditions. No doubt that the local coefficients will perform better on the BT simulation in general, although for some specific channels with central wavenumber around 1,700 to 1,800 cm^{-1}, the performance of local coefficients is slightly degraded. The comprehensive performances on BT simulation for each channel can be used together with other criteria in channel selection (J. Li & Han, 2017), for example, to keep those channels with BT simulation accuracy less dependent on the RTM training profiles and the atmospheric conditions.

5. Summary and Future Work

It should be noted that the fast RTM in clear skies has two components: the atmospheric radiation and the surface radiation. In this study, the focus is on the atmospheric radiative calculation, which is reflected by the atmospheric transmittance model. Having the specific transmittance model, any surface type with surface skin temperature and emissivity can be coupled together with transmittance model to generate the satellite radiance at top of the atmosphere for a given spectral IR channel. Detailed explanation of the components of top of the atmospheric radiance can be found in Saunders et al. (1999). In addition, the cloud scattering and absorption model can be coupled with clear-sky atmospheric transmittance model, along with surface contribution to form the fast RTM in cloudy skies (J. Li et al., 2005, 2017, 2004).

Evaluations of BT simulations using RTTOV GIIRS coefficients generated from global training profiles with OLS method, threshold value method, and WLS method, respectively, indicate the following:

1. Both the threshold value method and WLS have better performances on BT simulation accuracy than OLS method. The improvements are mainly found in the middlewave band, which is associated with strong water vapor absorption lines.
2. The WLS method has higher level of robustness than the threshold value method. The WLS + threshold method is the most recommended approach for generating RTTOV coefficients for any IR sensor.

The RTTOV GIIRS has been enhanced further by combining WLS + threshold method and the local training profiles. Evaluations of BT simulation accuracy from the global and local coefficients indicate the following:

3. RTTOV forward BT simulation errors for GIIRS are decreased overall by using the local coefficients. BT simulation accuracy from local coefficients has a 11.9%, 14.10%, 14.39%, and 5.06% improvement over the global coefficients for four different latitude regions, respectively. It implies that the local training profiles can enhance the RTTOV GIIRS accuracy especially in the nonextreme atmospheric conditions. There are more channels meeting the 0.05-K simulation accuracy standards by using local coefficients than using global coefficients accessed by independent testing profiles.
4. Major improvements from local coefficients are found in the longwave band. The largest ones occur in the regions around 800 cm^{-1} associated with CO_2 absorption lines and 1,050 cm^{-1} associated with O_3 lines. Since local training profiles can better represent the atmospheric conditions within the GIIRS observation coverage, especially for variables such as atmospheric temperature and ozone, the BT simulation accuracy from local coefficients is obviously higher than that from the global coefficients, especially for CO_2 and ozone absorption spectral regions.

Combined WLS + threshold method and the local training profiles is used for RTTOV GIIRS coefficients in this study, the approach can also be applied to RTTOV development for other geostationary sensors such as AGRI onboard FY-4 series, Advanced Baseline Imager onboard the GOES-R series, Advanced Himawari Imager onboard Himawari-8/-9, and InfraRed Sounder onboard the future Meteosat Third Generation series, for local weather applications such as assimilating high solution water vapor information from advanced geostationary imagers for improving heavy precipitation forecast (Wang et al., 2018). It should be noted that although local training profiles show superiority on global training profiles for GIIRS and could benefit regional weather related applications, the global coefficients are still useful for intercalibration between different geostationary IR sensors for consistent climate data record.

Acknowledgments
The RTTOV GIIRS version 11.2 local coefficients are publically available at ftp://ftp.ssec.wisc.edu/ABS/GIIRS_RTTOV11.2/rtcoef_fy4_1_giirs_local.dat to the research community for applications. This work was supported by the National Natural Science Foundation of China (grants 41305089 and 41675108) and GEO science program of NOAA NESDIS (grant NA15NES4320001). Hwan-Jin Song at the Seoul National University is thanked for good suggestions on selecting apodization function applied for GIIRS sounder. Xuan Feng is also thanked for providing the information on spectral characteristic of the GIIRS sounder. The SeeBor Version 5.0 database is from the Cooperative Institute for Meteorological Satellite Studies (CIMSS) of the University of Wisconsin-Madison (available at http://cimss.ssec.wisc.edu/training_data/). The global training profiles are achieved from the European Center of Medium-Range Weather Forecast (ECMWF; available at https://nwpsaf.eu/oldsite/deliverables/rtm/profile_datasets.html).

References

Bessho, K., Date, K., Hayashi, M., Ikeada, A., Imai, T., Inoue, H., et al. (2016). An introduction to Himawari-8/9—Japan's new-generation geostationary meteorological satellites. *Journal of the Meteorological Society of Japan*, *94*, 151–183. https://doi.org/10.2151/jmsj.2016-009

Borbas, E. E., Seemann, S. W., Huang, H.-L., Li, J., & Menzel, W. P. (2005). Global profile training database for satellite regression retrievals with estimates of skin temperature and emissivity. in *Proceedings of the XIV. International ATOVS study conference*, (pp. 763–770). Beijing, China: CIMSS: University of Wisconsin, Madison WI.

Chahine, M. T., Pagano, T. S., Aumann, H. H., Atlas, R., Barnet, C. D., Blaisdell, J., et al. (2006). AIRS: Improving weather forecasting and providing new data on greenhouse gases. *Bulletin of the American Meteorological Society*, *87*(7), 911–926. https://doi.org/10.1175/BAMS-87-7-911

Chen, Y., Han, Y., Van Delst, P., & Weng, F. (2010). On water vapor Jacobian in fast radiative transfer model. *Journal of Geophysical Research*, *115*(D12), D12303. https://doi.org/10.1029/2009jd013379

Chen, Y., Weng, F., Han, Y., & Liu, Q. (2008). Validation of the Community Radiative Transfer Model (CRTM) by using CloudSat data. *Journal of Geophysical Research*, *113*(D8), 2156–2202.

Chevallier, F., Sabatino, D. M., & McNally, A. P. (2006). Diverse profile datasets from the ECMWF 91-level short-range forecasts. *Report. No. NWPSAF-EC-TR-010*, NWP SAF, Exeter, U. K.

Clough, S. A., Kneizys, F. X., & Davis, R. W. (1989). Line shape and the water vapor continuum. *Atmospheric Research*, *23*(3-4), 229–241. https://doi.org/10.1016/0169-8095(89)90020-3

Clough, S. A., Kneizys, F. X., Rothman, L. S., & Gallery, W. O. (1981). Atmospheric spectral transmittance and radiance: FASCOD1B. *Proceedings of the SPIE*, *277*, 152–166. https://doi.org/10.1117/12.931914

Clough, S. A., Lacono, M. J., & Moncet, J.-L. (1992). Line-by-line calculation of atmospheric fluxes and cooling rates: Application to water vapor. *Journal of Geophysical Research*, *97*(D14), 15,761–15,785. https://doi.org/10.1029/92JD01419

Clough, S. A., Shephard, M. W., Mlawer, E. J., Delamere, J. S., Lacono, M. J., Cady-Pereira, K., Boukabara, S., et al. (2005). Atmospheric radiative transfer modeling: A summary of the AER codes, short communication. *Journal of Quantitative Spectroscopy and Radiative Transfer*, *91*(2), 233–244. https://doi.org/10.1016/j.jqsrt.2004.05.058

Eyre J. R. (1991). A fast radiative transfer model for satellite sounding systems. ECMWF Technical Memorandum 176.

Fox, J., & Weisberg, S. (2011). *An R companion to applied regression*. Thousand Oaks, CA: Sage Publications.

Goldberg, M. D., Cikanek, H. H., & Mehta, A. (2013). Joint Polar Satellite System: The United States next generation civilian polar-orbiting environmental satellite system. *Journal of Geophysical Research: Atmospheres*, *118*, 13,463–13,475. https://doi.org/10.1002/2013JD020389

Hilton, F., Armante, R., August, T., Barnet, C., Bouchard, A., Camy-Peyret, C., et al. (2012). Hyperspectral Earth observation from IASI: Five years of accomplishments. *Bulletin of the American Meteorological Society*, *93*(3), 347–370. https://doi.org/10.1175/BAMS-D-11-00027.1

Huber, P. J. (1964). Robust estimation of a location parameter. *Annals of Mathematical Statistics*, *35*(1), 73–101. https://doi.org/10.1214/aoms/1177703732

Le Marshall, J., Jung, J. A., Derber, J. C., Chahine, M. T., Treadon, R. E., Lord, S. J., et al. (2006). Improving global analysis and forecasting with AIRS. *Bulletin of the American Meteorological Society*, *87*(7), 891–895. https://doi.org/10.1175/BAMS-87-7-891

Li, J., & Han, W. (2017). A step forward toward effectively using hyperspectral IR sounding information in NWP. *Advances in Atmospheric Sciences*, *34*(11), 1263–1264. https://doi.org/10.1007/s00376-017-7167-2

Li, J., Huang, H.-L., Liu, C.-Y., Yang, P., Schmit, T. J., Wei, H., et al. (2005). Retrieval of cloud microphyiscal properties from MODIS and AIRS. *Journal of Applied Meteorology and Climatology*, *44*(10), 1526–1543. https://doi.org/10.1175/JAM2281.1

Li, J., Li, J., Otkin, J., Schmit, T. J., & Liu, C.-Y. (2011). Warning information in a preconvection environment from the geostationary advanced infrared sounding system—A simulation study using IHOP case. *Journal of Applied Meteorology and Climatology*, *50*(3), 776–783. https://doi.org/10.1175/2010JAMC2441.1

Li, J., Li, Z., Wang, P., Schmit, T. J., Bai, W., & Atlas, R. (2017). An efficient radiative transfer model for hyperspectral IR radiance simulation and applications under cloudy sky conditions. *Journal of Geophysical Research: Atmospheres*, *122*, 7600–7613. https://doi.org/10.1002/2016JD026273

Li, J., Liu, C.-Y., Zhang, P., & Schmit, T. J. (2012). Applications of full spatial resolution space-based advanced infrared soundings in the pre-convection environment. *Weather and Forecasting*, *27*(2), 515–524. https://doi.org/10.1175/WAF-D-10-05057.1

Li, J., Menzel, W. P., Zhang, W., Sun, F., Schmit, T. J., Gurka, J., & Weisz, E. (2004). Synergistic use of MODIS and AIRS in a variational retrieval of cloud parameters. *Journal of Applied Meteorology and Climatology*, *43*(11), 1619–1634. https://doi.org/10.1175/JAM2166.1

Li, J., Wang, P., Han, H., Li, J.-L., & Zheng, J. (2016). On the assimilation of satellite sounder data in cloudy skies in the numerical weather prediction models. *Journey of Meteorological Research*, *30*(2), 169–182. https://doi.org/10.1007/s13351-016-5114-2

Li, J., Wolf, W., Menzel, M. P., Zhang, W., Huang, H.-L., & Achtor, T. H. (2000). Global soundings of the atmosphere from ATOVS measurements: The algorithm and validation. *Journal of Applied Meteorology and Climatology*, *39*(8), 1248–1268. https://doi.org/10.1175/1520-0450(2000)039<1248:GSOTAF>2.0.CO;2

Li, Z., Li, J., Wang, P., Lim, A., Li, J., Schmit, T. J., Atlas, R., et al. (2018). Value-added impact of geostationary hyperspectral infrared sounders on local severe storm forecasts—Via a quick regional OSSE. *Advances in Atmospheric Sciences*, *35*(10), 1217–1230. https://doi.org/10.1007/s00376-018-8036-3

Matricardi, M. (2005), The inclusion of aerosols and clouds in RTIASI, the ECMWF fast radiative transfer model for the infrared atmospheric sounding interferometer, *ECMWF Technical Memorandum* 474, http://www.ecmwf.int/publications

Matricardi, M. (2007), An inter-comparison of line-by-line radiative transfer models, *ECMWF Technical Memorandum* 525, http://www.ecmwf.int/publications

Matricardi, M. (2008), The generation of RTTOV regression coefficients for IASI and AIRS using a new profile training set and a new line-by-line database, *ECMWF ECMWF Technical Memorandum* 564, http://www.ecmwf.int/publications

Matricardi, M. (2009). Technical note: An assessment of the accuracy of the RTTOV fast radiative transfer model using IASI data. *Atmospheric Chemistry and Physics*, *9*(18), 6899–6913. https://doi.org/10.5194/acp-9-6899-2009

Matricardi, M., Chevallier, F., & Tjemkes, S. (2001). An improved general fast radiative transfer model for the assimilation of radiance observations. *ECMWF Technical Memorandum* 345.

Matricardi, M., & Saunders, R. (1999). Fast radiative transfer model for simulation of infrared atmospheric sounding interferometer radiances. *Applied Optics*, *38*(27), 5679–5691. https://doi.org/10.1364/AO.38.005679

McNally, T., Bonavita, M., & Thépaut, J.-N. (2014). The role of satellite data in the forecasting of Hurricane Sandy. *Monthly Weather Review*, *142*(2), 634–646. https://doi.org/10.1175/MWR-D-13-00170.1

Menzel, W. P., & Purdom, J. F. W. (1994). Introducing GOES-I: The first of a new generation of geostationary operational environmental satellites. *Bulletin of the American Meteorological Society*, *75*(5), 757–781. https://doi.org/10.1175/1520-0477(1994)075<0757:IGITFO>2.0.CO;2

Menzel, W. P., Schmit, T. J., Zhang, P., & Li, J. (2018). Satellite based atmospheric infrared sounder development and applications. *Bulletin of the American Meteorological Society*, *99*(3), 583–603. https://doi.org/10.1175/BAMS-D-16-0293.1

Saunders, R. W., Matricardi, M., & Brunel, P. (1999). An improved fast radiative transfer model for assimilation of satellite radiance observations. *Quarterly Journal of the Royal Meteorological Society*, *125*(556), 1407–1425. https://doi.org/10.1002/qj.1999.49712555615

Schmit, T. J., Gunshor, M. M., Menzel, W. P., Gurka, J., Li, J., & Bachmeier, S. (2005). Introducing the next-generation advanced baseline imager (ABI) on GOES-R. *Bulletin of the American Meteorological Society*, *86*(8), 1079–1096. https://doi.org/10.1175/BAMS-86-8-1079

Schmit, T. J., Li, J., Ackerman, S. A., & Gurka, J. J. (2009). High spectral and high temporal resolution infrared measurements from geostationary orbit. *Journal of. Atmospheric and Oceanic Technology*, *26*(11), 2273–2292. https://doi.org/10.1175/2009JTECHA1248.1

Smith, W. L., Woolf, H. M., Hayden, C. M., Wark, D. Q., & McMillin, L. M. (1979). The TIROS-N operational vertical sounder. *Bulletin of the American Meteorological Society*, *60*, 1177–1187.

Wang, P., Li, J., Goldberg, M., Schmit, T. J., Lim, A. H. N., Li, Z., Han, H., et al. (2015). Assimilation of thermodynamic information from advanced IR sounders under partially cloudy skies for regional NWP. *Journal of Geophysical Research: Atmospheres*, *120*, 5469–5484. https://doi.org/10.1002/2014JD022976

Wang, P., Li, J., Li, J. L., Li, Z., Schmit, T. J., & Bai, W. (2014). Advanced infrared sounder subpixel cloud detection with imagers and its impact on radiance assimilation in NWP. *Geophysical Research Letters*, *41*, 1773–1780. https://doi.org/10.1002/2013GL059067

Wang, P., Li, J., Li, Z., Lim, A. H. N., Li, J.-L., Schmit, T. J., & Goldberg, M. D. (2017). The impact of Cross-track Infrared Sounder (CrIS) Cloud-Cleared Radiances on Hurricane Joaquin (2015) and Matthew (2016) Forecasts. *Journey of Geophysical Research - Atmospheres*, *122*(24), 13,201–13,218. https://doi.org/10.1002/2017JD027515

Wang, P., Li, J., Lu, B., Schmit, T. J., Lu, J., Lee, Y.-K., Li, J., et al. (2018). Impact of moisture information from Advanced Himawari Imager measurements on heavy precipitation forecasts in a regional NWP model. *Journal of Geophysical Research: Atmospheres*, *123*(11), 6022–6038. https://doi.org/10.1029/2017JD028012

Yang, J., Zhang, Z., Wei, C., Lu, F., & Guo, Q. (2017). Introducing the new generation of Chinese geostationary weather satellites, Fengyun-4. *Bulletin of the American Meteorological Society*, *98*(8), 1637–1658. https://doi.org/10.1175/BAMS-D-16-0065.1

Zhang, J., Li, Z., Li, J., & Li, J. (2014). Ensemble retrieval of atmospheric temperature profiles from AIRS. *Advances in Atmospheric Sciences*, *31*(3), 559–569. https://doi.org/10.1007/s00376-013-3094-z

Zhang, K., Wu, C., & Li, J. (2016). Retrieval of atmospheric temperature and moisture vertical profiles from satellite advanced infrared radiances with a new regularization parameter selecting method. *Journal of Meteorological Research*, *30*(3), 356–370.https://doi.org/10.1007/s13351-016-6025-y